

# Combining a thermal-imaging diagnostic with an existing imaging VISAR diagnostic at the National Ignition Facility (NIF)

Robert M. Malone<sup>\*a</sup>, John R. Celeste<sup>b</sup>, Peter M. Celliers<sup>b</sup>, Brent C. Frogget<sup>a</sup>, Robert L. Guyton<sup>c</sup>, Morris I. Kaufman<sup>a</sup>, Tony L. Lee<sup>b</sup>, Brian J. MacGowan<sup>b</sup>, Edmund W. Ng<sup>b</sup>, Imants P. Reinbachs<sup>c</sup>, Ronald B. Robinson<sup>b</sup>, Lynn G. Seppala<sup>b</sup>, Tom W. Tunnell<sup>a</sup>, Phillip W. Watts<sup>c</sup>

<sup>a</sup>Bechtel Nevada, PO Box 809, 182 East Gate Dr., Los Alamos, NM 87544;

<sup>b</sup>Lawrence Livermore National Laboratory, PO Box 808, Livermore, CA 94551;

<sup>c</sup>Bechtel Nevada, 161 S. Vasco Rd, Livermore, CA 94551

## ABSTRACT

Optical diagnostics are currently being designed to analyze high-energy density physics experiments at the National Ignition Facility (NIF). Two independent line-imaging Velocity Interferometer System for Any Reflector (VISAR) interferometers have been fielded to measure shock velocities, breakout times, and emission of targets having sizes of 1–5 mm. An 8-inch-diameter, fused silica triplet lens collects light at  $f/3$  inside the 30-foot-diameter NIF vacuum chamber. VISAR recordings use a 659.5-nm probe laser. By adding a specially coated beam splitter to the interferometer table, light at wavelengths from 540 to 645 nm is split into a thermal-imaging diagnostic. Because fused silica lenses are used in the first triplet relay, the intermediate image planes for different wavelengths separate by considerable distances. A corrector lens on the interferometer table reunites these separated wavelength planes to provide a good image. Thermal imaging collects light at  $f/5$  from a 2-mm object placed at Target Chamber Center (TCC). Streak cameras perform VISAR and thermal-imaging recording. All optical lenses are on kinematic mounts so that pointing accuracy of the optical axis may be checked. Counter-propagating laser beams (orange and red) are used to align both diagnostics. The red alignment laser is selected to be at the 50 percent reflection point of the beam splitter. This alignment laser is introduced at the recording streak cameras for both diagnostics and passes through this special beam splitter on its way into the NIF vacuum chamber.

**Keywords:** VISAR, interferometer, optical relay, National Ignition Facility (NIF), streak camera

## 1. INTRODUCTION

VISAR<sup>1,2</sup> measures the velocity of a moving surface by recording its Doppler wavelength shift. The NIF VISAR diagnostic is a primary means for timing the shocks induced into an ignition capsule.<sup>3,4</sup> Figure 1 shows the 90-315 port location of an imaging VISAR system fielded to collect images inside a 33-foot-diameter vacuum target chamber at NIF. Earlier VISAR work was done at the 90-45 port.<sup>5,6,7</sup> Drive laser beams (not shown) enter into the NIF target

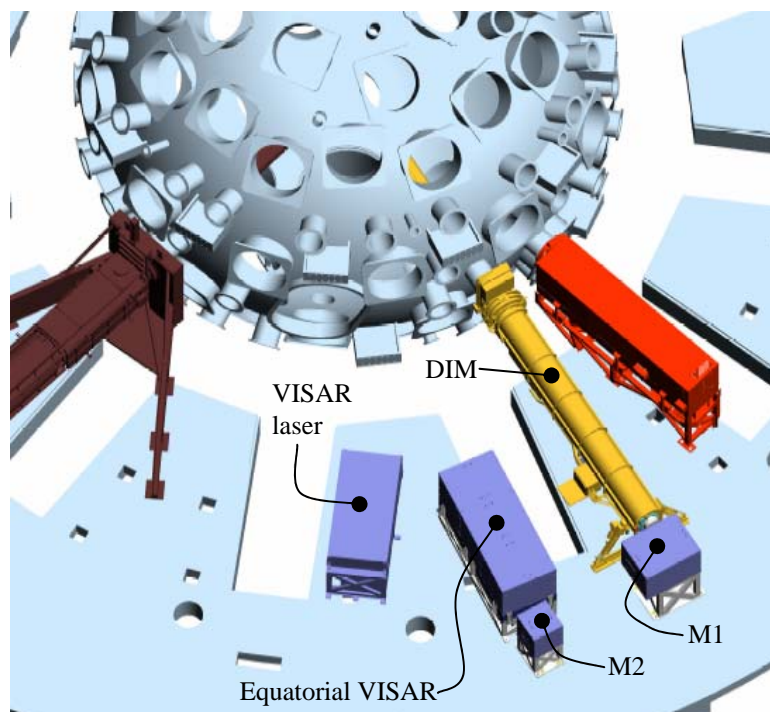


Fig. 1. VISAR next to 90-315 port of the NIF target chamber.

\* malonerm@nv.doe.gov; phone 1 505 663-2014; fax 1 505 663-2003

chamber through its largest ports and are focused onto a sample target. Currently, VISAR utilizes one of the chamber's equatorial ports and uses a Diagnostic Instrumentation Manipulator (DIM) which is designed for multiple users. VISAR DIM cart hardware, including lenses and baffles, is divided into two sections and is loaded into the DIM like a torpedo. It is designed to be compatible with existing DIM hardware designs.<sup>6,7</sup> The original VISAR installation was for the 90-45 chamber port. Because of an interfering support pillar, the long axis of the interferometer table was perpendicular to the DIM.<sup>5,6,7</sup> This newer layout, required by the 90-315 chamber port, has the interferometer table rotated by 90 degrees.

Figure 2 shows the ray trace layout of this imaging VISAR diagnostic. A protective laser curtain (not shown) encloses both the laser and interferometer tables. Optics and mounting hardware inside the DIM are removable. L3/M1 and M2 boxes, pinned to the floor, are detachable so that other diagnostics may use this same DIM location. Interferometer and laser tables are stationary. All enclosures for the DIM vacuum gate valve, vacuum window, L3/M1 box, M2 box, interferometer table, and probe laser table have safety interlock switches.

The light from the TCC is collected by a triplet lens (L1) and exits the DIM through a 2-inch-thick vacuum window. An intermediate image, formed inside the DIM, is picked up by a doublet lens (L3) placed in front of the first turning mirror (M1). A second turning mirror (M2) lowers the optical path to the interferometer table height. Because of the many optical elements required by the two interferometers, the recording streak cameras are mounted on a second level. A dove prism is located between the two optical breadboards to allow image rotation.

To minimize damage to expensive optical components, turning mirrors M1 and M2 (and turning mirrors M8 and M9 placed in front of the streak cameras) have special coatings that do not reflect 1053-nm, 527-nm, or 351-nm NIF drive laser wavelengths. All optical elements from the TCC to the beam splitter BS1 on the interferometer table (including mirrors M1 and M2) are fused silica. This material minimizes radiation darkening caused by the intense X-rays from some NIF experiments. Narrowband filters (3 nm) and cutoff filters are placed behind dove prisms (where the relayed light is almost collimated) protecting the streak camera data from NIF drive lasers.

The special reflective broadband coatings of these turning mirrors, which reject the unwanted NIF drive laser wavelengths, allow for other thermal-emission light produced by the target to enter onto the interferometer table (Figure 3). A diagnostic has been designed to collect a 105-nm range of wavelengths at a spectral wavelength region not contaminated by the VISAR probe laser. We chose the range from 540 nm to 645 nm. Light will be split off from the optical system using a specially coated beam splitter (BS5, shown in Figure 7) that transmits the VISAR light and reflects the 540- to 645-nm band. No loss of VISAR intensity occurs. Using a band of wavelengths longer than that of

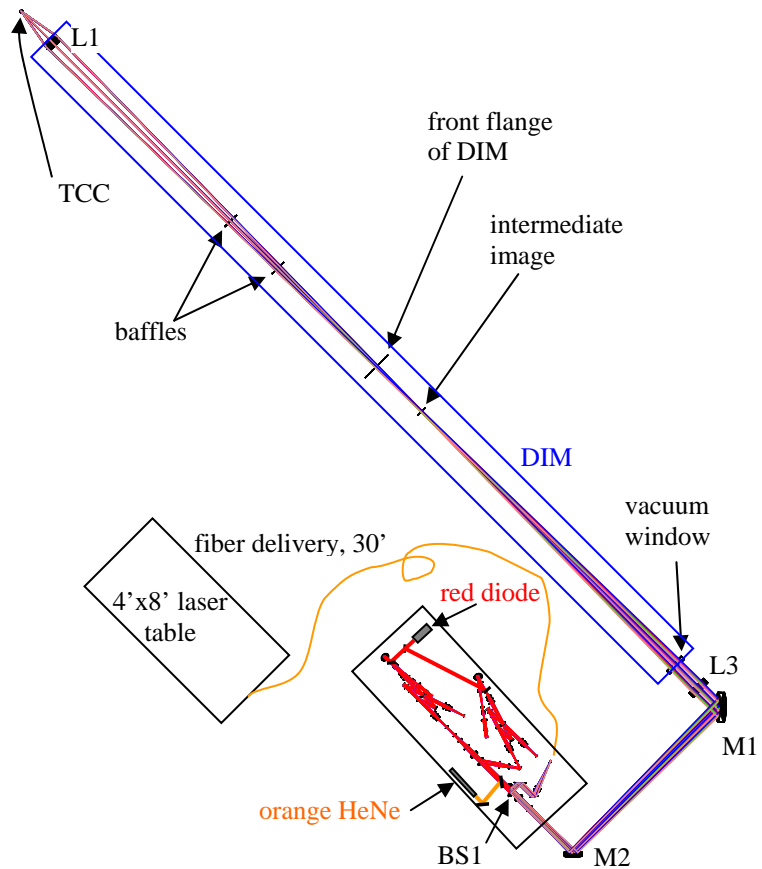


Fig. 2. Labeling of the VISAR optical relay system. The red diode laser, introduced in front of the streak cameras, is sent all the way to TCC. The orange HeNe is sent to slits of the streak cameras.

the 659.5-nm VISAR laser would have reduced sensitivity from the recording streak camera (S-20 extended red response).

## 2. OPTICAL DESIGN PROBLEM

The requirement is to undo the axial color separation caused by the fused silica optical elements. Because the triplet lens L1 is in a radiation zone, its elements are made of fused silica which is acceptable for VISAR but allows no color correction for a band of wavelengths. Figure 4 shows (with exaggerated scaling) light passing through the DIM at four discrete wavelengths. The object size and its  $f/\#$  are different than that of VISAR, so here the baffles have little effect on this diagnostic. Other stray light baffles are inserted on the interferometer table. At the first intermediate image plane, the object is magnified by 11.2X, and the axial color separation is 25.5 inches. The L3 doublet is also fused silica, so the problem worsens before any correction lens can be applied.

The thermal emission from the target is unpolarized light. The special beam splitter (BS5, not shown until Figure 7) that will separate the thermal-emission light must have a sharp transition between reflection and transmission. This beam splitter is positioned in front of BS5. Because a dichroic beam splitter tilted at 45 degrees has significant separation in its reflectivity between S and P polarization states, we minimized the tilt angle to 10 degrees. This angle sets the locations for the turning mirrors that routed the thermal emission light to the streak camera located on the second level of the interferometer enclosure.

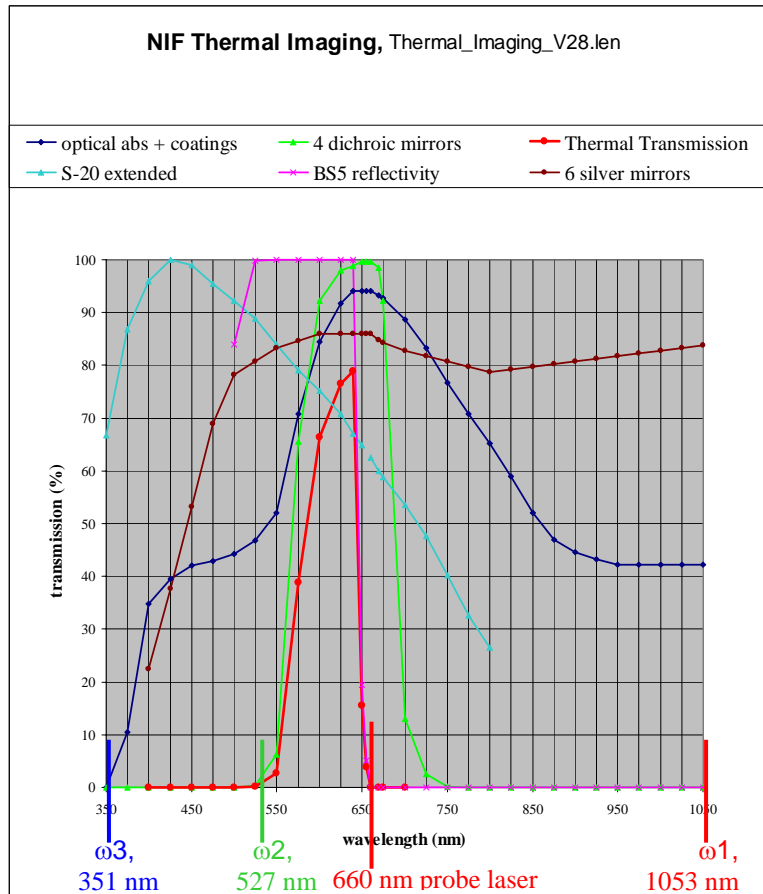


Fig. 3. Transmission curves for VISAR imaging. The 660-nm probe laser is positioned away from the NIF drive lasers.

## 3. CORRECTOR LENS DESIGN

The design makes great use of global optimization to provide the best lens form to solve the wavelength problem. The distance from intermediate image plane IP4 to the streak camera at first was allowed to vary. We used Fourier relay doublets (F2/BK7) borrowed from the existing VISAR to collect the light from intermediate image plane IP4 and send it to the streak camera slit position. By allowing the wavelength range to increase from 0.2 nm to 10 nm, the relay lenses were allowed to change, but the MTF worsened. When the glass was allowed to vary, the MTF improved. The best lens form was chosen from the global optimization runs. To gain better performance, we added two more lenses. During global optimization, the design criteria used was to select the lens form where there was a minimum amount of ray bending on the glass surfaces. After many global optimization cycles, the best performer was a six-element lens group, shown in Figure 5, where real glasses<sup>5</sup> have been selected. This six-element lens has many surfaces that would generate background glow from ghost reflections. We were able to resolve 1 part in 100 at the streak camera slit over a 60-nm wavelength range.

Next, we derived another design, using five elements. We found a solution in which we could couple surface curvatures so that cemented doublets could be used. The final lens design appears in Figure 6. Using identical doublet

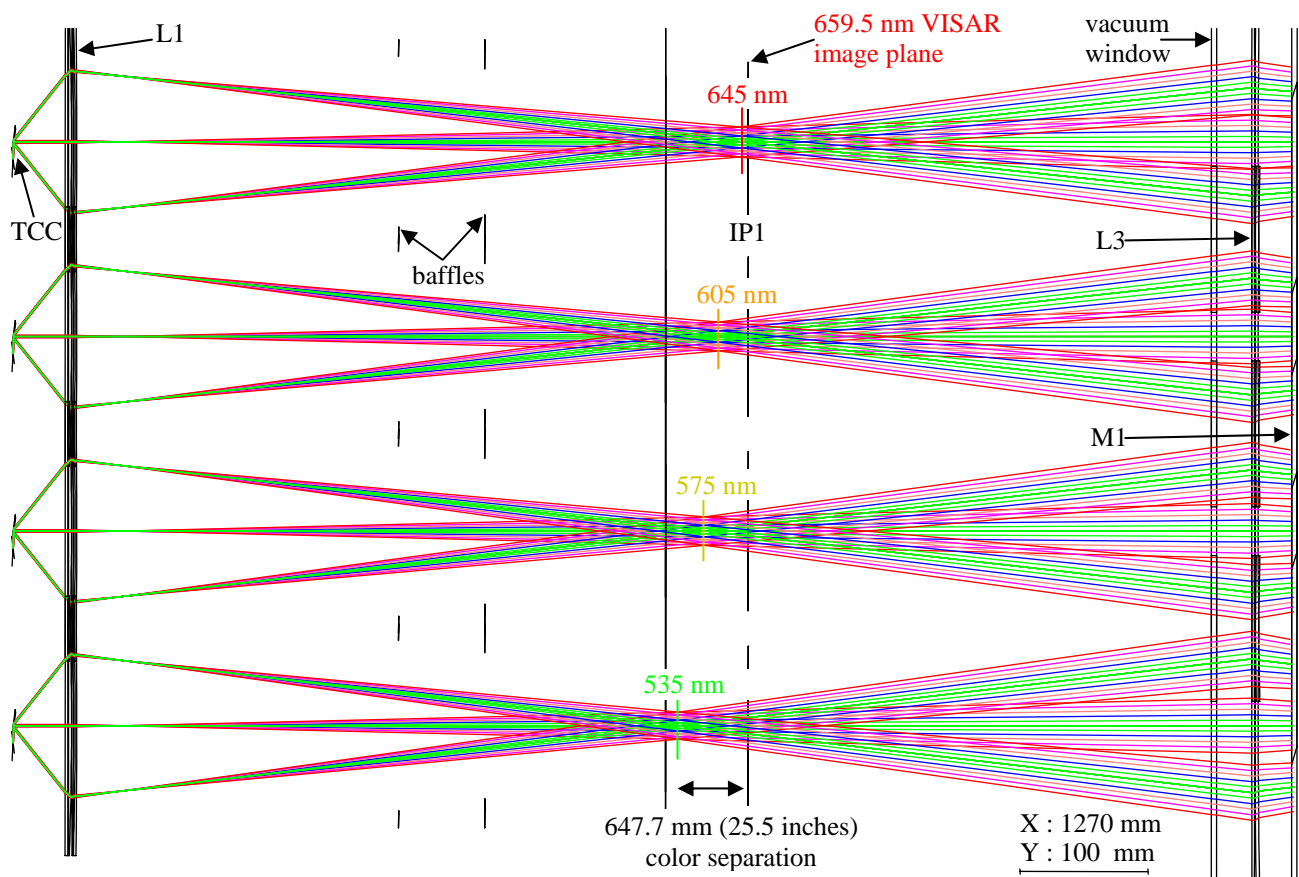


Fig. 4. Color separation at intermediate image plane IP1. The 8-in diameter fused silica elements used at the position of lens L1 (a blast window and a triplet lens) cause the shift versus wavelength. L1 center thickness is 3.5 in. Note: the Y-axis has been greatly expanded to see these image planes.

lenses reduced the cost. This lens form is much longer, but reducing the number of glass surfaces from twelve to six will reduce background light recorded by the streak camera.

We did not have a spare L10 relay lens from the VISAR optics, which formed the second intermediate image plane (IP2) location (see Figure 7). Using commercial lenses to reduce costs, we redesigned this relay lens using BK7 and SF2 glasses. This allowed the wavelength correction to start with this lens. Without this L10c correcting lens, required resolution limited the band of wavelengths to about 75 nm. Using both L10c and L15 correcting lenses, we were able to resolve 1 part in 100 at the streak camera slit over a 105-nm wavelength range.

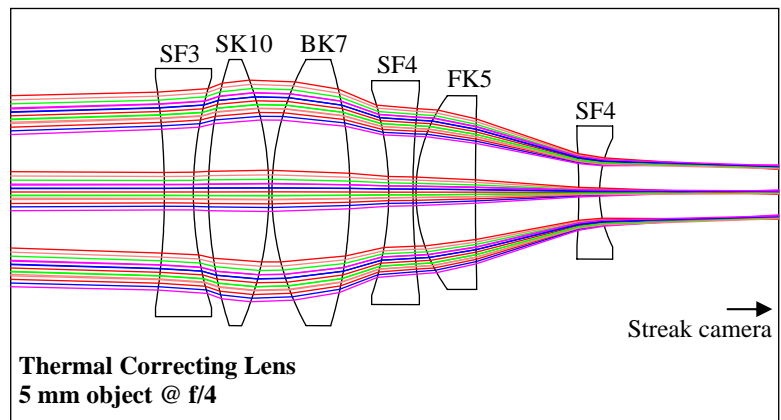


Fig. 5. Prototype six-element thermal correcting lens.

#### 4. OPTICAL LAYOUT

The thermal-imaging optical system must not interfere with VISAR, a primary NIF diagnostic. Additionally, this new diagnostic is not allowed to attenuate any light sent to the VISAR interferometers. Thus, a special beam splitter must be designed to transmit 100 percent of the VISAR light, reflect the thermal-imaging spectrum, and relay it to its own streak camera. The resulting optical layout, which requires mirrors at compound angles, uses a dove prism for correct image rotation.

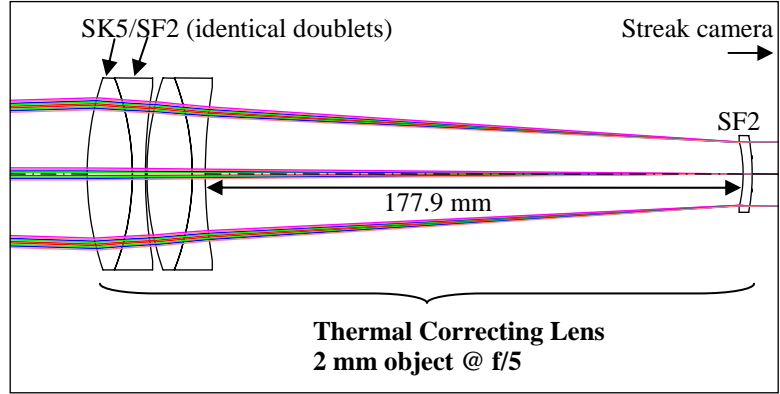


Fig. 6. Final five-element thermal correcting lens.

Figure 7 offers a perspective view of the thermal-imaging diagnostic (green rays) newly added to the existing VISAR table. All recording streak cameras are mounted on an upper level (not shown). The probe laser beam path and two interferometers beam paths combine at beam splitter BS1. Beam splitter BS2 divides the VISAR light into two separate interferometers. Beam splitter BS5, used to separate out thermal emission wavelengths, is positioned where the light is nearly collimated.

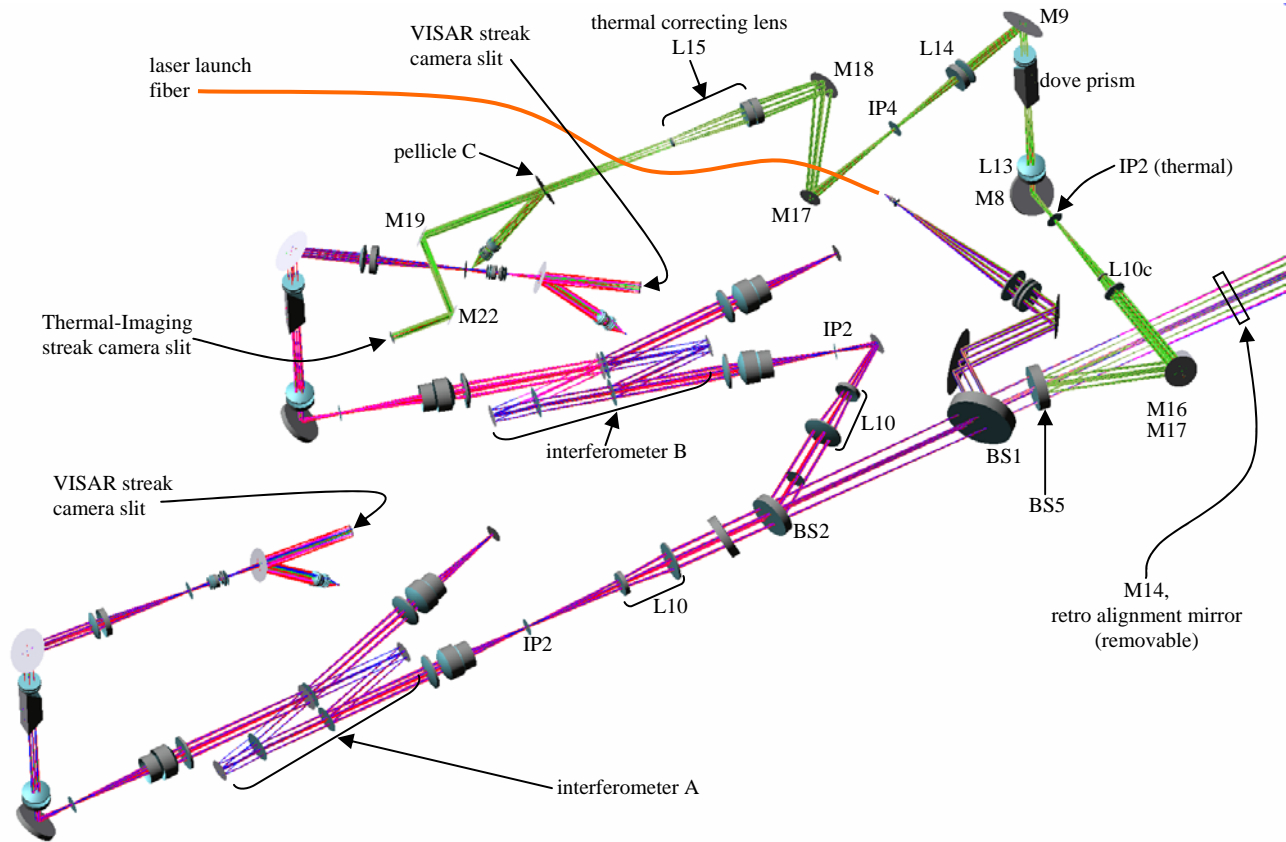


Fig. 7. Perspective view of interferometer enclosure. (Breadboard levels are not shown.)

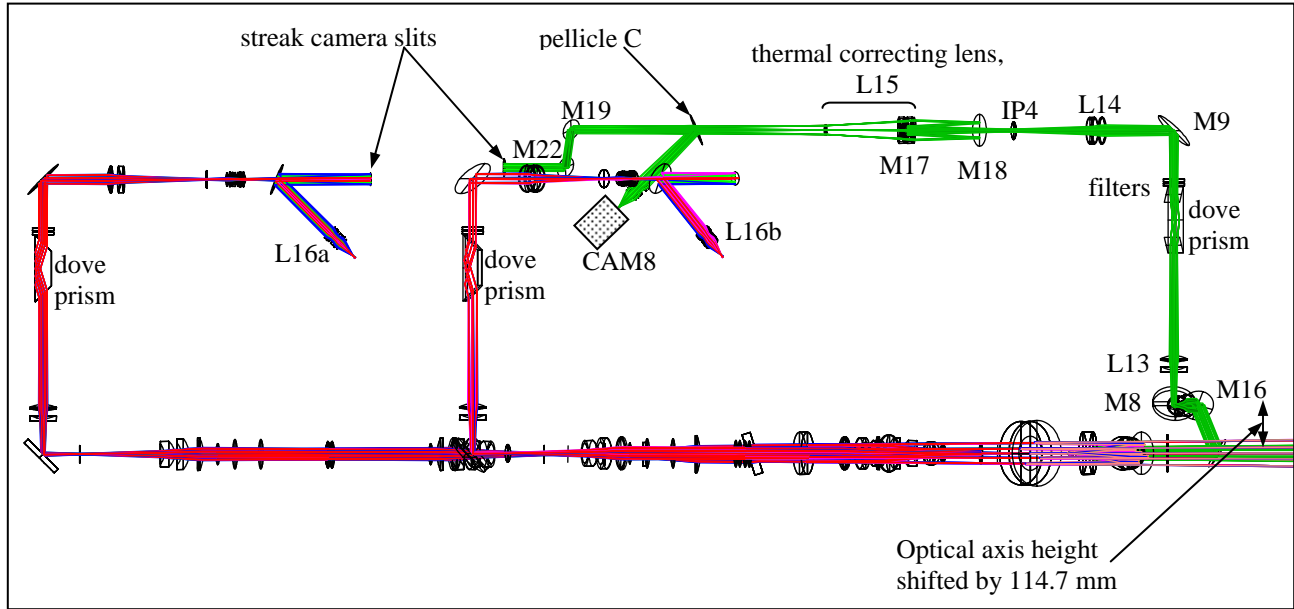


Fig. 8. Side view shows some of the many optical components inside of the interferometer enclosure. Optical components are mounted onto two stacked breadboards. (Breadboard levels are not shown.)

A side view of this system appears in Figure 8. Two optical breadboards (not shown) support many optical elements inside the interferometer enclosure. The two interferometers are on the lower level and all streak camera recording is performed on the second level. A CCD monitor camera (CAM8) is used to archive image registration of target pattern features relative to the streak camera slit. Pellicle C, placed before the streak camera slit, is used only temporarily for setup and calibration data.

## 5. THERMAL-IMAGING DIAGNOSTIC ALIGNMENT

L15 is an unusual relay lens because its object (intermediate image plane IP4) is placed at a different distance depending on its wavelength. Figure 9 shows that the distance from the lens to the streak camera slit remains constant over the wavelength range. However, the object distance changes by 57.3 mm over the 105-nm wavelength range. This distance would have been larger if we did not start the color correction with the up stream L10c lens. Only the ray tracing from the last intermediate image plane (IP4) to the streak camera slit appears in Figure 9 (shown without 4 folding mirrors).

Proper focus adjustment of lens L15 can only be made using a laser wavelength, since the position of intermediate image plane IP4 depends on wavelength. Using white light with a narrowband filter produces a blurry image. (For the VISAR diagnostic, using white light with a narrowband filter allows for optimal focus because speckle is eliminated.)

We selected a red diode laser to have a wavelength (652.7 nm) at the 50 percent reflection point of beam splitter BS5. Its light is inserted just in front of the streak camera and travels backward through the optics on its way to the target at TCC. Another orange laser is inserted (using flip mirrors) after BS5 for both VISAR and the thermal imaging system. Its light passes through the dove prism on its way to the streak camera slits. All optical elements are on kinematic bases so that they can be easily removed to establish the correct optical axis. The advantages of a two-color laser alignment scheme were discussed in reference 6 and 7.

Figure 10 is a top view of the interferometer enclosure. The position of IP2 on the thermal system has to be shifted depending on which laser provides its illumination. Inserting mirror M14 will allow some of the 652.7 nm alignment laser to reflect backwards into the thermal imaging system and illuminate a resolution pattern placed at IP2. The orange laser (612 nm) can also illuminate this same resolution pattern. This allows us to achieve proper focus of the L10c and L15 correcting lenses at two different wavelengths. The shift of IP2 position for these two wavelengths is 15.7 mm.

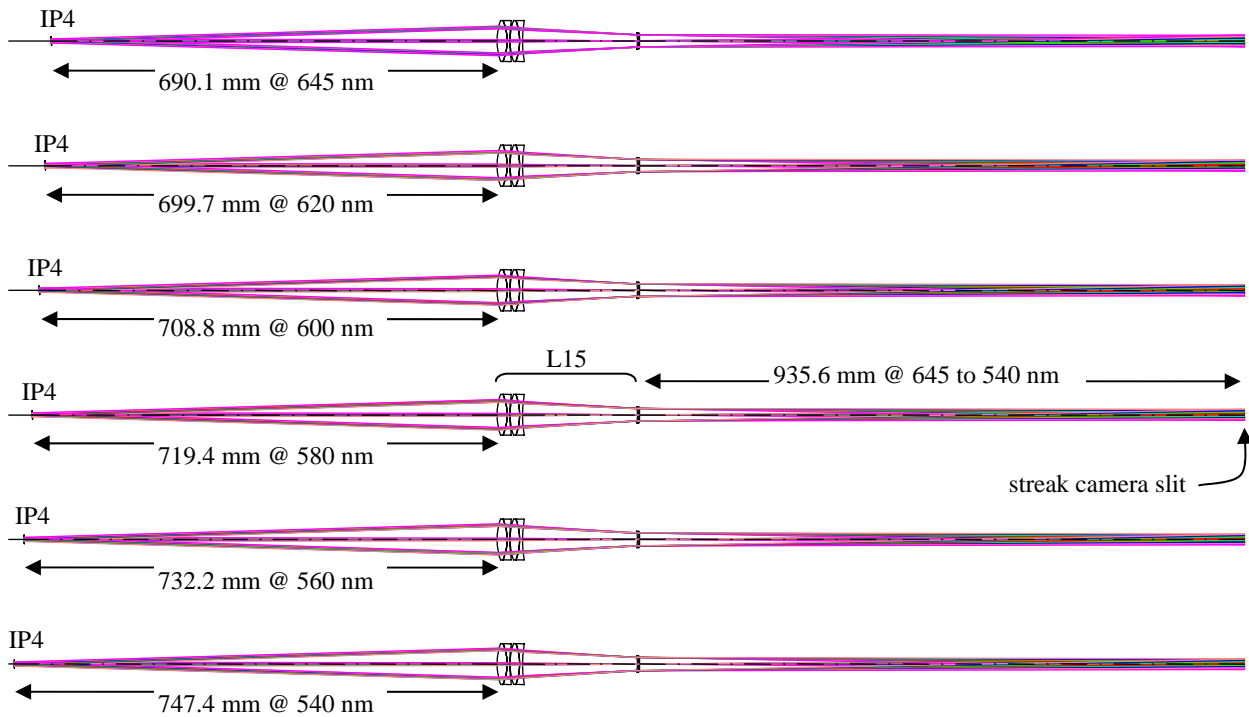


Fig. 9. Intermediate image plane IP4 (located before the thermal correcting lens, L15) is at a different location for different wavelengths. Distance from lens L15 to the streak camera slit is unchanged. This unfolded geometry does not include the 4 folding mirrors that are shown in Figures 7 and 8.

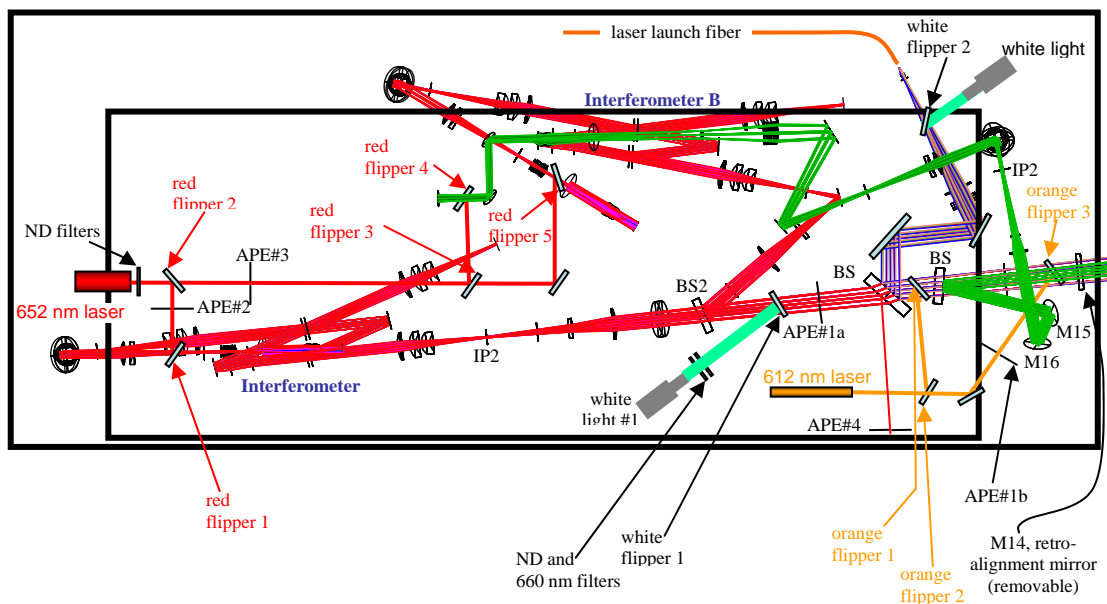


Fig. 10. Layout of laser alignment system. The red (652 nm) laser is inserted just before streak cameras and passes backward through the optical systems to APE#4 and also TCC. The orange (612 nm) laser is inserted either before BS1 or before BS2 and passes forwards through the optical systems to the streak camera slits.

## 6. CONCLUSION

Our team has designed for NIF an optical diagnostic using the same front-end optics as VISAR. We have developed a correcting lens that undoes the chromatic aberrations produced by the fused silica front-end optics. A specially designed beam splitter ensures that VISAR light is not attenuated. Using a 105-nm wavelength band, we can resolve 1 part in 100 across a 2-mm-sized object with our recording streak camera. No cross talk of light exists between the VISAR and the thermal-imaging diagnostics. A dove prism allows for rotating the object's image and the streak camera slit selects a line profile of this object. The full image could also be sent to a framing camera to record a movie.

## REFERENCES

1. L. M. Barker and R. E. Hollenbach, "Laser interferometer for measuring high velocities of any reflecting surface," *J. Appl. Phys.* **43**, 4669 (1972); L. M. Barker and K. W. Schuler, "Correction to the velocity-per-fringe relationship for the VISAR interferometer," *J. Appl. Phys.* **45**, 3692 (1974).
2. D. D. Bloomquist and S. A. Sheffield, "Optically recording interferometer for velocity measurements with sub nanosecond resolution," *J. Appl. Phys.* **54**, 1717 (1983).
3. P.M. Celliers, G. W. Collins, L. B. Da Silva, D. M. Gold, R. C. Cauble, R. J. Wallace, M. E. Foord, and B. A. Hammel, "Shock-Induced Transformation of Liquid Deuterium into a Metallic Fluid," *Phys. Rev. Lett.* **84**, 5564–5567 (2000).
4. D. H. Munro, P. M. Celliers, G. W. Collins, D. M. Gold, L. B. Da Silva, S. W. Haan, R. C. Cauble, B. A. Hammel, and W. W. Hsing, "Shock timing technique for the National Ignition Facility," *Physics of Plasmas* **8**, 2245 (2001).
5. R.M. Malone, B.C. Frogget, M.I. Kaufman, P.W. Watts, P.M. Bell, J.R. Celeste, T.L. Lee, "Design of an imaging VISAR diagnostic for the National Ignition Facility (NIF)," *SPIE Proc.* **5173**, 26–37 (2003).
6. R.M. Malone, G.A. Capelle, B.C. Frogget, R.L. Guyton, M.I. Kaufman, G.A. Lare, T.W. Tunnell, P.W. Watts, J.R. Bower, J.R. Celeste, P.M. Celliers, T.L. Lee, B.J. MacGowan, S. Montelongo, E.W. Ng, T.L. Thomas, "Fielding of an imaging VISAR diagnostic at the National Ignition Facility (NIF)," *SPIE Proc.* **5523**, 148–157 (2004).
7. R. M. Malone, J. R. Bower, D. K. Bradley, G. A. Capelle, J. R. Celeste, P. M. Celliers, G. W. Collins, M. J. Eckart, J. H. Eggert, B. C. Frogget, R. L. Guyton, D. G. Hicks, M. I. Kaufman, B. J. MacGowan, S. Montelongo, E. W. Ng, R. B. Robinson, T. W. Tunnell, P. W. Watts, P. G. Zapata, "Imaging VISAR diagnostic for the National Ignition Facility (NIF)," *SPIE Proc.* **5580**, 505–516 (2004).

**Copyright.** This manuscript has been authored by Bechtel Nevada under Contract No. DE-AC08-96NV11718 with the U.S. Department of Energy. The United States Government retains and the publisher, by accepting the article for publication, acknowledges that the United States Government retains a non-exclusive, paid-up, irrevocable, world-wide license to publish or reproduce the published form of this manuscript, or allow others to do so, for United States Government purposes.

**Disclaimer.** This report was prepared as an account of work sponsored by an agency of the U.S. Government. Neither the U.S. Government nor any agency thereof, nor any of their employees, nor any of their contractors, subcontractors or their employees, makes any warranty or representation, express or implied, or assumes any legal liability or responsibility for the accuracy, completeness, or usefulness of any information, apparatus, product, or process disclosed, or represents that its use would not infringe privately own rights. Reference herein to any specific commercial product, process, or service by trade name, trademark, manufacturer, or otherwise, does not necessarily constitute or imply its endorsement, recommendation, or favoring by the U.S. Government or any agency thereof. The views and opinions of authors expressed herein do not necessarily state or reflect those of the U.S. Government or any agency thereof.